SUB-GRID SCALE MODELING OF AIR TOXICS CONCENTRATIONS NEAR ROADWAYS

Prakash Karamchandani*, Kristen Lohman and Christian Seigneur
Atmospheric and Environmental Research Inc., San Ramon, CA, USA

1. INTRODUCTION

Population exposure to hazardous air pollutants (HAPs), also known as air toxics, is an important health concern. Air toxics exposure is generally higher in urban areas than in rural areas and tends to be localized around the emission sources. For example, measurements of toxic air pollution levels near a busy freeway in Los Angeles showed that exposures near the freeway were up to 10 times greater than those at background locations and dropped to background levels within 300 m downwind of the freeway (Zhu et al., 2002a). Any modeling approach used to calculate the exposure impacts of air toxics must be able to capture this variability in exposure levels.

Gaussian plume dispersion models have been used extensively in air toxics modeling to simulate the near-field impacts of emissions from point, area and mobile sources. However, these models assume steady-state conditions for calculating downwind concentrations; furthermore, they cannot treat atmospheric chemical transformations (except simple first-order decay) and, therefore, are not suitable for many air toxics, which are chemically reactive. On the other hand, three-dimensional grid models, that are often used for applications involving a large number of sources and reactive pollutants, are not able to capture the subgrid-scale variability in concentrations near a source because of their coarse resolution (typically from 4 km to tens of kilometers). Thus, simulating the atmospheric transport and fate of chemically reactive toxic air pollutants requires the use of models that can handle non-steady-state conditions and reactive pollutants as well as resolve the sub-grid scale features of emissions from point and line sources.

Several air toxics modeling studies have pointed out the possible limitations associated with a coarse spatial resolution of air toxics emissions and concentrations. For example, the Neighborhood Assessment Program of the California Air Resources Board recommends a combination of a 3-D grid model and local plume dispersion models to assess air toxics concentrations (e.g., Isakov and Venkatram, 2006). Ching and co-workers (Ching et al., 2006) have developed an approach where they account for sub-grid spatial variability using the results of simulations conducted with a finer spatial resolution. The pros and cons of each of these approaches have been discussed by Seigneur (2004) and Touma et al. (2006).

We describe here a Plume-in-Grid (PiG) modeling approach that differs from the previous approaches by combining the 3-D grid-based modeling approach with a local scale modeling approach within a single model. The PiG approach is preferable to the one where two models are used separately (a grid model for regional pollution and a dispersion model for local pollution) because issues arise for reactive pollutants when recombining the results of the two model simulations (e.g., Seigneur et al., 2002).

The PiG model used in this study consists of a reactive plume model (SCICHEM) that is embedded within a three-dimensional grid model (CMAQ), providing the capability of capturing the local variability in concentrations near a source as well as treating the chemical transformations of reactive species. The model, referred to as CMAQ-APT (CMAQ with Advanced Plume Treatment), has previously been applied to point sources for ozone (Karamchandani et al., 2002; Vijayaraghavan et al., 2006), particulate matter (Karamchandani et al., 2006a) and mercury (Karamchandani et al., 2006b).

In the proof-of-concept study presented here, we have adapted CMAQ-APT to develop a prototype model to simulate near-roadway concentrations due to mobile emissions from a busy interstate highway in New York City. We also perform a qualitative comparison of model results with measured concentration profiles available near a major highway in Los Angeles (no measurements were available for New York City). For this demonstration study, we focus only on mobile emissions of carbon monoxide (CO) and benzene.

**Corresponding author:* Prakash Karamchandani, Atmospheric and Environmental Research, Inc., 2682 Bishop Drive, Suite 120, San Ramon, CA 94583-4282; e-mail: pkaramch@aer.com

2. MODELING APPROACH

For this initial application, the chemistry and aerosol modules of CMAQ-APT were deactivated and CO and benzene were treated as chemically-inert species; this is an appropriate approximation for these chemical species at the spatial scales considered here (less than 500 m from the emission source). SCICHEM, the plume component of CMAQ-APT, has traditionally been used to simulate point source emissions, but the framework allows the use of any source, as long as the relevant source characteristics are correctly specified. For this study, the roadway emissions that were simulated with SCICHEM were specified as adjacent elongated area sources, where each source represented a road segment. The following section provides additional details on the treatment of roadway emissions.

The model outputs include both the three-dimensional grid cell concentrations, as well as the puff incremental concentrations (i.e., the fraction of the total concentration in the puff that is above background). The concentration at any receptor location is then the sum of the grid cell average concentration of the cell containing the receptor and the perturbation concentrations of the puffs impacting that receptor. Thus, the model outputs contain information to calculate concentrations at discrete receptor locations, allowing us to predict concentrations at the subgrid-scale. A post-processor was developed to calculate the modeled concentrations of CO and benzene at selected receptor points perpendicular to the roadway. Each set of receptors is located at various distances along the busiest sections of the roadway, as described in the following section.

3. MODEL APPLICATION

The model was applied to the July 11-15, 1999 period of the NARSTO/Northeast program. The NARSTO modeling domain consists of two nested grids (see Figure 1). The outer domain has a horizontal resolution of 12 km while the inner domain has a horizontal resolution of 4 km. For this study, we used the inner 4 km domain, which includes New York City, New Jersey and Washington, D.C. The domain consists of 99 x 135 grid cells in the horizontal and 13 layers with variable resolution in the vertical. The boundary conditions for the simulation were obtained from the 12 km domain results from another study (Seigneur et al., 2003).

Below, we describe how roadway emissions were developed for the plume component of the model. We also describe the selection of receptor locations near the roadway for presenting the model results.

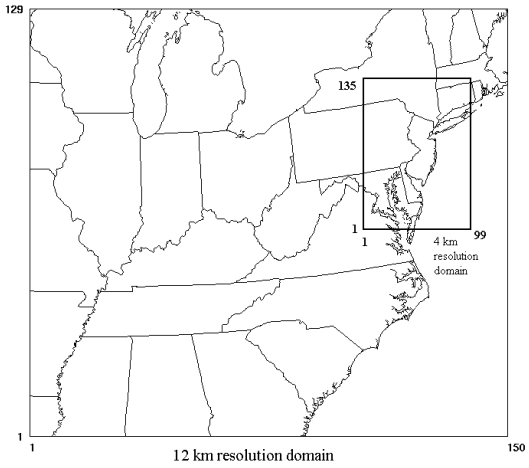

Fig. 1. Modeling domains for the NARSTO-Northeast simulation. The inner domain (4 km horizontal resolution) was used in this study.

3.1 Roadway Emissions

We selected a busy highway in the modeling domain based on the annual average daily traffic counts for various highways in the domain, Traffic count information was obtained by downloading traffic data from the Bureau of Transportation Statistics in the form of GIS files from the National Highway Planning Network (NHPN) (BTS, 2007). The data in the NHPN include both locations of the highway segments (county, latitude, longitude, and length) and also the annual average daily traffic count from the 2002 Highway Performance Monitoring System.

We chose a section of Interstate 278 (I278), which passes through all five boroughs of New York City (see Figure 2). The length of the selected section of the highway is about 50 km. This section of the highway was divided into several smaller segments, with each segment specified as a separate area source to the embedded plume model. Each segment is approximately 30 m long, based on the assumption that the highway width is 30 m and on the constraint that the initial size of the source must be less than or equal to the highway width.

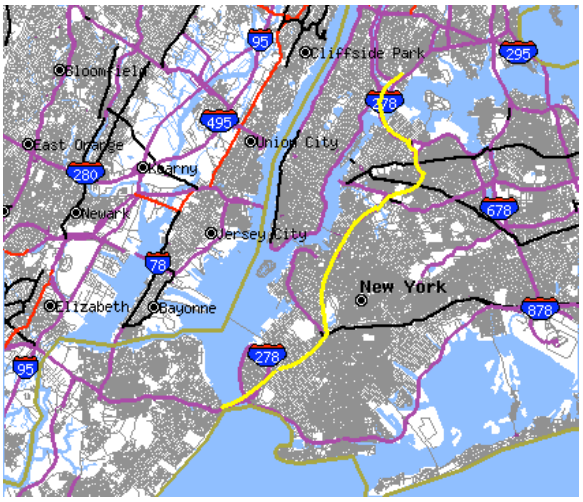

Fig. 2. Map showing section of Interstate 278 (in yellow) selected for this study.

The benzene and CO emissions data were obtained from a pre-existing SMOKE input file. Emissions from this file were available by county and Source Classification Code (SCC). The emissions for all SCC corresponding to highway traffic were summed for each county. A factor was created for I278 emissions in each county by dividing the I278 vehicle-miles (traffic count x segment length) traveled in that county by the total highway vehicle-miles traveled for the county. The vehicle-miles factor was multiplied by the highway emissions for each county to determine the total annual emissions of benzene and CO due to vehicle emissions on I278.

A list of highway segments was generated that covered the length of the selected section of I278. These segments were taken from the NHPN file. The segments were then split up by county, and each segment received a percentage of the county-wide I278 emissions calculated above. The percentage was based on the vehicle-miles traveled for that segment as compared to the total vehicle-miles traveled for I278 in that county. Once the emissions were calculated for each segment of each county, the segments were broken up into smaller (roughly 30 m) segments and the emissions were divided proportionately into each small segment. Next, the SMOKE temporal profiles were applied. There are three temporal profiles: monthly, day-of-week, and hourly. These profiles apply a fraction of the annual emissions to each hour of each day of the year. The profiles reflect changes in human activity over the course of the year, week, and day.

The total number of 30 m segments was nearly 1700. Each segment was specified as an emissions source for the plume component of the model. These emissions were subtracted from the three-dimensional emission file used by the host model to avoid double-counting of emissions. This “background” file (the file with all emissions except mobile emissions from I278) was created as follows. Each segment of I278 was assigned to its corresponding grid cell. The emissions for each grid cell for each hour were then aggregated. Then, the original gridded CMAQ emission file was read in. For each grid cell that contained some portion of I278, the roadway emissions corresponding to that grid cell were removed from the gridded CMAQ emissions.

3.2 Receptor Locations

The following considerations were used in placing the receptors for post-processing the model outputs. First, the receptors should be located along one of the busiest stretches of the roadway. Second, the receptors should be located such that the spatial variability in concentrations could be captured. The largest spatial variabilities are expected when the winds are perpendicular to the roadway. Thus, we chose a section of the roadway that was not only busy but also exhibited significant curvature, increasing the likelihood of locating receptors in the along-wind direction.

Several sets of receptors were placed along the selected section of the roadway. Figure 3 shows a line sketch of the highway with the receptor transects marked. There are 29 sets of receptors. The receptors in each transect are placed perpendicularly to the roadway at 10, 20, 30, 40, 50, 100, 200, 300, 400, and 500 m from the center of the roadway in both directions. Each transect is about 300 m apart. The section of I278 along which receptors are placed begins in Queens after the intersection of I278 with the Long Island Expressway/I495 and with Route 25. It includes the Triborough Bridge in Manhattan and the last transect is located just before I278 intersects Interstates 87 and 895 in the Bronx. Figure 3 also identifies 5 transects that are used in the discussion of results below.

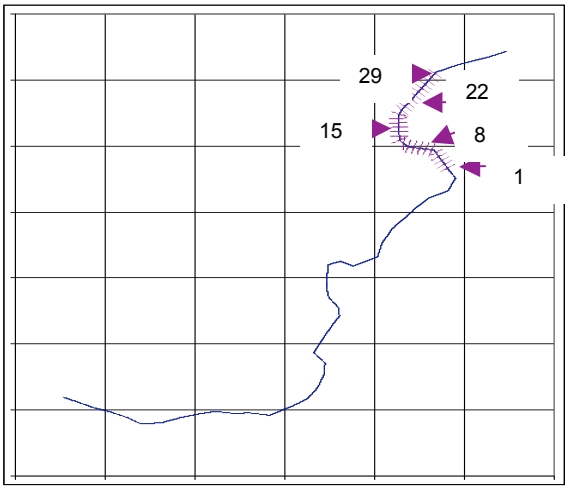

Fig. 3. Locations of 29 receptor transects along a section of I278 in Queens and Manhattan. The 5 transects identified in the figure (Transects 1, 8, 15, 22 and 29) are used for presenting the model results.

4. RESULTS

In this section, we show across-roadway concentration profiles of CO for selected hours and receptor transects. Although benzene was also simulated, the profiles for benzene are similar to those for CO and are not shown here. The results are shown for Transect 1, Transect 8, Transect 15, Transect 22 and Transect 29 (see Figure 3 for the locations of these transects) for hours during which the maximum CO perturbation (from the background or grid-cell value) was simulated for each transect. The spacing between each of these transects is about 2.1 km. Because the wind flow is not exactly perpendicular to the roadway and the freeway direction curves around (see Figure 3), there are generally no clearly defined upwind and downwind sides of the roadway; nevertheless, we define below the upwind side as the side of the roadway that has the lower concentrations and the downwind side as the one that has the greater concentrations.

Transect 1 is in Queens just after the intersection of I278 with Route 25 (Queens Boulevard). Figure 4 shows the concentration profiles across the roadway at this location at 6 pm local time (EDT) on July 12, 1995. The blue line represents the grid-cell averaged CO concentration from a grid model only simulation (i.e., in a separate CMAQ simulation, all sources, including mobile sources on I278 were treated in the grid model). All the receptor points fall in the same grid cell (each grid cell is 4 km by 4 km), so there is only one value for the grid-cell averaged concentration. The red circles are the CO concentrations from the plume-in-grid simulation in which the I278 mobile sources are treated with the embedded puff model in CMAQ.

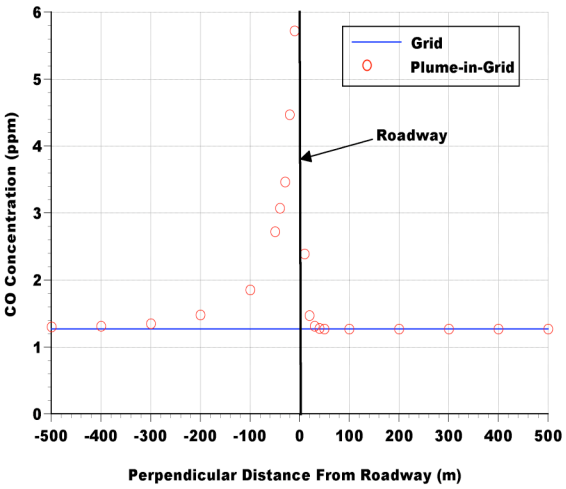

Fig. 4. Across-roadway CO concentration profile for Transect 1 at 6 pm local time on July 12, 1995.

From Figure 4, we see that the CO concentrations are greater southwest of the roadway (left side of the figure) than northeast of the roadway (right of the roadway) because the wind is blowing from the north. The peak CO concentration is nearly 6 ppm at 10 m from the center of the roadway, more than 4 times the grid-cell value of about 1.3 ppb. The concentration drops very rapidly upwind and it is about equal to the urban background concentration at 40 m from the center of the roadway; downwind, it drops rapidly to about 4.5 ppm and 3.5 ppm at 20 m and 30 m from the roadway, respectively. At 300 m from the roadway, the concentration is only slightly larger than the grid-cell value.

Figure 5 shows the results for Transect 8 at 8 am local time on July 12, 1995. This transect is approximately at the location where I278 intersects and joins the Grand Central Parkway. The results are qualitatively similar to those for Transect 1 except that the difference between the upwind (left side of the figure) and downwind (right side of the figure) sides of the roadway is not as clearly defined as in the previous case. The peak CO concentration of nearly 10 ppm at 10 m from the center of the roadway is slightly more than 4 times the grid-cell value of about 2.4 ppm. On the downwind side, the concentrations drop exponentially with increasing distance from the roadway, reaching background levels at about 300 m from the roadway. On the upwind side, the CO

concentrations drop to the urban background level within about 100 m.

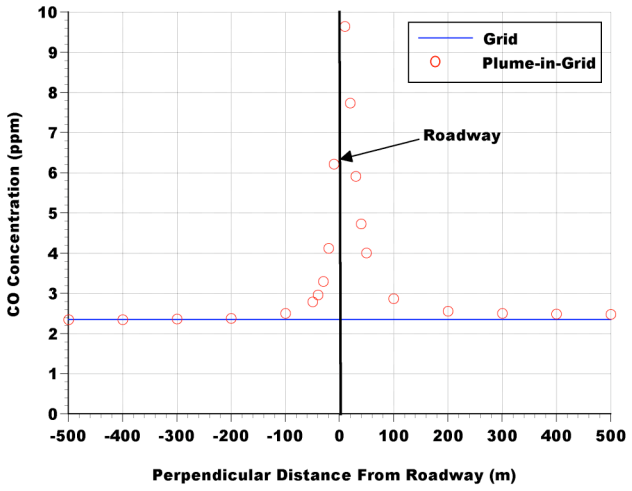

Fig. 5. Across-roadway CO concentration profile for Transcect 8 at 8 am local time on July 12, 1995.

Transect 15 is located just after I278 becomes the Triborough Bridge and enters the outskirts of Manhattan over Wards Island Park. Figure 6 shows the results for this transect at 12 noon on July 13, 1995. The peak CO concentration of 38 ppm at 10 m from the roadway is more than 7 times the grid-cell value of 5 ppm, but drops rapidly to background levels at 200 m from the roadway on the downwind side and at 100 m from the roadway on the upwind side.

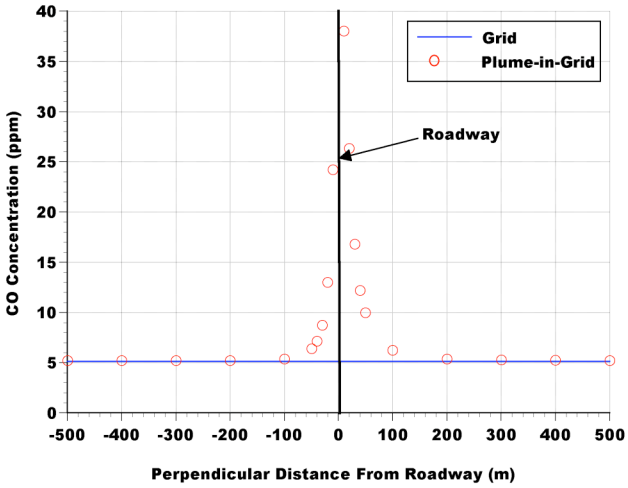

Fig. 6. Across-roadway CO concentration profile for Transect 15 at 12 pm local time on July 13, 1995.

The next transect presented here (Transect 22) is on the Triborough Bridge portion of I278 just over Randalls Island Park. Figure 7 shows the across-roadway CO concentration profile for this transect at 7 am local time on July 13, 1995. The peak CO concentration near the roadway is 26 ppm, about 5 times the grid-cell value. The concentrations drop to about 7 ppm at 500 m from the roadway center on the downwind side. It drops to the background level of 5 ppm within 200 m from the roadway center on the upwind side.

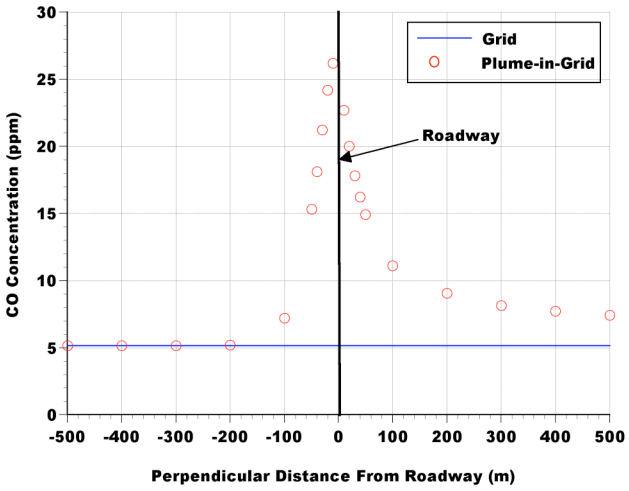

Fig. 7. Across-roadway CO concentration profile for Transect 22 at 7 am local time on July 13, 1995.

The last transect (Transect 29) is at the interchange of I278 with I87, where I278 becomes the Bruckner Expressway and enters the Bronx. The results for this transect at 8 am on July 13, 1995 are shown in Figure 8. The peak CO concentration at 10 m from the roadway is about 23 ppm, more than a factor of 4 higher than the grid-cell value. The concentration drops to the background level of 5 ppm within 200 m from the roadway center; however, the concentration drops only to 9 ppm at 500 m on the downwind side, still nearly a factor of two higher than the background level.

The results presented here are qualitatively consistent with measurements made by Zhu et al. (2002a; 2002b) on two different freeways in the Los Angeles area in the summer and fall of 2001. They found that peak CO concentration levels near the freeways were up to 10 times larger than background levels and dropped exponentially to background levels within 300 m of the roadway.

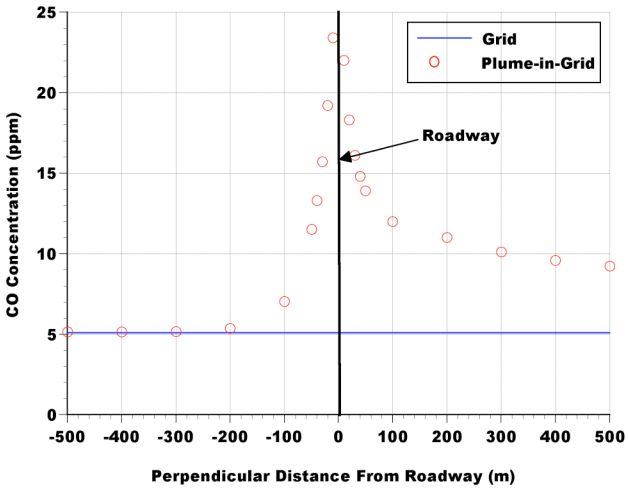

Fig. 8. Across-roadway CO concentration profile for Transect 29 at 8 am local time on July 13, 1995.

5. SUMMARY

This proof-of-concept study has shown that it is possible to adapt available modeling tools to conduct subgrid-scale modeling of toxic air pollutants for estimating population exposure to these species.

This study focused on one type of source, namely vehicles, and assumed that the emitted species (CO and benzene) were unreactive. Also, for practical reasons, the application of the model presented here used an existing data base available to us for the eastern United States. However, there were no roadway measurements available to directly evaluate the model, and we could only perform a qualitative comparison with measurements made in Southern California.

The next step is to extend this modeling approach to other sources, and to use the prototype model developed here for a variety of species with their atmospheric chemistry. The model can be applied to other regions of the country, such as Southern California, Houston, TX or the Raleigh-Durham area, NC, where measurements of air toxics are available to conduct a quantitative model performance evaluation.

6. REFERENCES

BTS, 2007. http://www.bts.gov/publications/national_transportation_atlas_database/2006

Ching, J., J. Herwehe and J. Swall, 2006. On joint deterministic grid modeling and sub-grid variability conceptual framework for model evaluation, *Atmos. Environ.*, **40**, 4935-4945.

Isakov, V. and A. Venkatram, 2006. Resolving neighborhood scale in air toxics modeling: a case study in Wilmington, CA, *J. Air Waste Manage. Assoc.*, **56**, 559-568.

Karamchandani, P., C. Seigneur, K. Vijayaraghavan and S.-Y. Wu, 2002. Development and application of a state-of-the-science plume-in-grid model, *J. Geophys. Res.*, **107**, 4403-4415.

Karamchandani, P., C. Seigneur and K. Vijayaraghavan, 2004. Development and testing of an advanced Plume-in-Grid PM model, *AWMA Visibility Specialty Conference*, October 26-29, 2004, Asheville, NC.

Karamchandani, P., K. Vijayaraghavan, S.-Y. Chen, C. Seigneur and E.S. Edgerton, 2006a. Plume-in-grid modeling for particulate matter, *Atmos. Environ.*, **40**, 7280-7297.

Karamchandani, P., K. Vijayaraghavan, S.-Y. Chen and C. Seigneur, 2006b. Plume-in-grid modeling for PM and mercury, *5th Annual CMAS Conference*, October 16-18, 2006, Chapel Hill, NC.

Seigneur, C., B. Pun, K. Lohman and S.-Y. Wu, 2002. Air Toxics Modeling, Report A-42-1, http://www.crcao.com.

Seigneur, C., B. Pun, K. Lohman and S.-Y. Wu, 2003. Regional modeling of the atmospheric fate and transport of benzene and diesel particles, *Environ. Sci. Technol.*, **37**, 5236-5246.

Seigneur, C., 2004. Air toxics modeling: state of the science, current challenges and future prospects, *Coordinating Research Council (CRC) Mobile Source Air Toxics Workshop*, 1-2 December 2004, Scottsdale, Arizona.

Touma, J.S., V. Isakov, J. Ching and C. Seigneur, 2006. Air quality modeling of hazardous pollutants: current status and future directions, *J. Air Waste Manage. Assoc.*, **56**, 547-558.

Vijayraghavan, K., P. Karamchandani and C. Seigneur, 2006. Plume-in-grid modeling of summer air pollution in Central California, *Atmos. Environ.*, **40**, 5097-5109.

Zhu, Y., W.C. Hinds, S. Kim and C. Sioutas, 2002a. Concentration and size distribution of ultrafine particles near a major highway, *J. Air Waste Manage. Assoc.*, **52**, 1032-1042.

Zhu, Y., W.C. Hinds, S. Kim, S. Shen and C. Sioutas, 2002b. Study of ultrafine particles near a major highway with heavy-duty diesel traffic, *Atmos. Environ.*, **36**, 4323-4335.